

Ecological and evolutionary implications of starvation and body size

1 **Justin D. Yeakel * †‡, Christopher P. Kempes †, and Sidney Redner †§**

4 *School of Natural Science, University of California Merced, Merced, CA, †The Santa Fe Institute, Santa Fe, NM, §Department of Physics, Boston University, Boston
5 MA, and ‡To whom correspondence should be addressed: jdyeakel@gmail.com

6 Submitted to Proceedings of the National Academy of Sciences of the United States of America

7 **This is the abstract.** No it isn't. It's merely a placeholder.

8 foraging | starvation | reproduction

9 Introduction

10 The behavioral ecology of most, if not all, organisms is influ-
11 enced by the energetic state of individuals, which directly influ-
12 ences how organisms invest reserves in uncertain environments.
13 Such behaviors are generally manifested as trade-offs between
14 investing in somatic maintenance and growth or allocating en-
15 ergy towards reproduction [1, 2, 3]. The timing of these be-
16 haviors responds to selective pressure, as the choice of the in-
17 vestment impacts future fitness! [4]. The influence of resource
18 limitation on an organism's ability to maintain its nutritional
19 stores may lead to repeated delays or shifts in reproduction over
20 the course of an organism's life.

21 The life history of most species is typically comprised of (a)
22 somatic growth and maintenance and (b) reproduction. The
23 balance between these two activities is often conditioned on
24 resource availability [5]. For example, reindeer invest less in
25 calves born after harsh winters (when the mother's energetic
26 state is depleted) than in calves born after moderate winters [6].
27 Many bird species invest differently in broods during periods
28 of resource scarcity compared to normal periods [7, 8], some-
29 times delaying or even foregoing reproduction for a breeding
30 season [1, 9, 10]. Even freshwater and marine zooplankton have
31 been observed to avoid reproduction under nutritional stress
32 [11], and those that do reproduce have lower survival rates [2].
33 Organisms may also separate maintenance and growth from re-
34 production over space and time: many salmonids, birds, and
35 some mammals return to migratory breeding grounds to repro-
36 duce after one or multiple seasons in resource-rich environments
37 where they accumulate nutritional reserves [12, 13, 14].

38 Physiological mechanisms also play an important role in reg-
39 ulating reproductive expenditures during periods of resource
40 limitation. Diverse mammals (47 species in 10 families) ex-
41 hibit delayed implantation, whereby females postpone fetal
42 development (blastocyst implantation) until times where nu-
43 tritional reserves can be accumulated [15, 16]. Many other
44 many species (including humans) suffer irregular menstrual cy-
45 cling and higher abortion rates during periods of nutritional
46 stress [17, 18]. In the extreme case of unicellular organisms,
47 nutrition is unavoidably linked to reproduction because the nu-
48 tritional state of the cell regulates all aspects of the cell cycle
49 [19]. The existence of so many independently evolved mechan-
50 isms across such a diverse suite of organisms highlights the im-
51 portance and universality of the fundamental tradeoff between
52 somatic and reproductive investment. However the dynamic
53 implications of these constraints are unknown.

54 Though straightforward conceptually, incorporating the en-
55 ergetic dynamics of individuals [20] into a population-level
56 framework [20, 21] presents numerous mathematical obsta-
57 cles [22]. An alternative approach involves modeling the
58 macroscale relations that guide somatic versus reproductive
59 investment in a consumer-resource system. For example,
60 macroscale Lotka-Volterra models assume that the growth rate

61 of the consumer population depends on resource density, thus
62 *implicitly* incorporating the requirement of resource availability
63 for reproduction [23].

64 In this work, we adopt an alternative approach in which re-
65 source limitation and the subsequent effect of starvation is ac-
66 counted for *explicitly*. Namely, only individuals with sufficient
67 energetic reserves can reproduce. Such a constraint leads to
68 reproductive time lags due to some members of the population
69 starving and then recovering. Additionally, we incorporate the
70 idea that reproduction is strongly constrained allometrically [3],
71 and is not generally linearly related to resource density. As we
72 shall show, these constraints influence the ensuing population
73 dynamics in dramatic ways.

74 Nutritional-state-structured model (NSM)

75 We begin by defining a minimal Nutritional-State-
76 structured population Model (NSM), where the consumer pop-
77 ulation is divided into two energetic states: (a) an energetically
78 replete (full) state F , where the consumer reproduces at a con-
79 stant rate λ , and (b) an energetically deficient (hungry) state
80 H , where the consumer does not reproduce but dies at rate μ .
81 The underlying resource R evolves by logistic growth with an
82 intrinsic growth rate α and a carrying capacity equal to one.
83 Consumers transition from the full state F to the hungry state
84 H by starvation at rate σ and also in proportion to the absence
85 of resources $(1 - R)$. Conversely, consumers recover from state
86 H to state F at rate ρ and in proportion to R . Resources are
87 also eaten by the consumers—at rate ρ by hungry consumers
88 and at rate $\beta < \rho$ by full consumers. This inequality accounts
89 for hungry consumers requiring more resources to rebuild body
90 weight.

90 In the mean-field approximation, in which the consumers
91 and resources are perfectly mixed, their densities evolve accord-
92 ing to the rate equations

$$\begin{aligned}\dot{F} &= \lambda F + \rho RH - \sigma(1 - R)F, \\ \dot{H} &= \sigma(1 - R)F - \rho RH - \mu H, \\ \dot{R} &= \alpha R(1 - R) - R(\rho H + \beta F).\end{aligned}\quad [1]$$

93 Notice that the total consumer density $F + H$ evolves accord-
94 ing to $\dot{F} + \dot{H} = \lambda F - \mu H$. This resembles the equation of
95 motion for the predator density in the classic Lotka-Volterra
96 model, except that the resource density does not appear in the

Reserved for Publication Footnotes

99 growth term. As discussed above, the attributes of reproduction 158 3). If σ is too large, mortality due to starvation depletes the
 100 and mortality have been explicitly apportioned to the full 159 consumer population, resulting in a lower steady state density
 101 and hungry consumers, respectively, so that the growth in the 160 for the consumer and a higher steady state density for the re-
 102 total density is decoupled from the resource density. 161 source.

103 Equation [1] has three fixed points: two trivial fixed points 162 Whereas the rate of consumer growth defines a hard bound
 104 at $(F^*, H^*, R^*) = (0, 0, 0)$ and $(0, 0, 1)$, and one non-trivial, 163 of biological feasibility (the TC bifurcation), the rate of starva-
 105 internal fixed point at 164 tion thus determines the sensitivity of the consumer population
 165 to changes in resource density. While higher rates of starva-
 166 tion result in lower steady state population size – increasing
 167 the risk of stochastic extinction – lower rates of starvation re-
 168 sult in a system poised near either the TC or Hopf bifurcation,
 169 which will lead to elimination of the resource or the develop-
 170 ment of cyclic oscillations, respectively. Which bifurcation is
 171 approached is wholly dependent on the rate of recovery: if it
 172 is high, then cyclic dynamics will develop; if it is low, resource
 173 extinction becomes increasingly likely.

$$\begin{aligned} F^* &= \frac{\alpha\lambda\mu(\mu + \rho)}{(\lambda\rho + \mu\sigma)(\lambda\rho + \mu\beta)}, \\ H^* &= \frac{\alpha\lambda^2(\mu + \rho)}{(\lambda\rho + \mu\sigma)(\lambda\rho + \mu\beta)}, \\ R^* &= \frac{\mu(\sigma - \lambda)}{\lambda\rho + \mu\sigma}. \end{aligned} \quad [2]$$

106 If this unique internal fixed point is stable, it will be the global 162 attractor for all population trajectories for any set of initial
 107 conditions where the resource and consumer densities are both 163 non zero. Stability of the fixed point is determined by the Jaco-
 108 bian Matrix \mathbf{J} , where each matrix element J_{ij} equals $\partial\dot{X}_i/\partial X_j$ 164 when evaluated at the internal fixed point, and \mathbf{X} is the vector
 109 (F, H, R) . If the parameters in Eq. [1] are such that the real 165 part of the largest eigenvalue of \mathbf{J} is negative, then the system is
 110 stable with respect to small perturbations from the fixed point. 166

111 A fundamental constraint on the NSM is that the repro- 167 duction rate λ must be less than the starvation rate σ . If 168 across the range of mammals for each of the key parameters
 112 $\lambda > \sigma$, the fixed point value of R^* has an unphysical nega- 169 tive value. Moreover, when the resource density $R = 0$, the 170 rate equation for F gives exponential growth for $\lambda > \sigma$. The 171 condition $\sigma = \lambda$ represents a transcritical (TC) bifurcation that 172 demarcates the physical and unphysical regimes. The biological 173 meaning of the constraint $\lambda < \sigma$ is simple—the rate at which 174 an organism loses mass due to a lack of resources 175 is generally much faster than the rate of reproduction. As we 176 will discuss below, this inequality is a natural consequence of 177 allometric constraints [3] for organisms within observed body 178 size ranges (Fig. 2).

113 In the physical regime where $\lambda < \sigma$, the fixed point [2] may 179 either be a stable node or a stable spiral node.

114 In addition to the bound defined by the TC bifurcation, 180 oscillating or cyclic dynamics present an implicit constraint to 181 persistence by increasing extinction risk due to stochastic ef- 182 fects. In continuous-time systems, a stable limit cycle arises 183 when a pair of complex conjugate eigenvalues crosses the imag- 184 inary axis to attain positive real parts [28]. This condition, 185 mated by $\lambda = \lambda_0 M^{\eta-1}$. This relationship is derived from the 186 known as a Hopf bifurcation, is defined by $\text{Det}(\mathbf{S}) = 0$, where 187 \mathbf{S} is the Sylvester matrix, which is composed of the coefficients 188 of the characteristic polynomial describing the Jacobian [29].

115 Moreover, as a non-cyclic stable system nears the Hopf bi- 189 furcation, transient or decaying cycles can grow in magnitude, 190 [a and b notation — these parameters are easily measured
 116 despite the existence of a positive, non-cyclic, steady state den- 191 bioenergetic parameters which are often approximately invari-
 117 perturbation [30], even the onset of transient cycles that de- 192 ant across organisms of vastly different size. Our notation seeks
 118 cay over time can increase the risk of extinction [31, 32, 33], 193 on a small number of free parameters.] where E_m is the energy
 119 such that the distance of a system from the Hopf bifurcation is 194 needed to synthesize a unit of mass, B_m is the metabolic rate
 120 relevant to persistence.

121 The NSM exhibits both non-cyclic as well as cyclic dynam- 195 ics, and which behavior dominates depends strongly on the rate 196 of starvation σ relative to the rate of recovery ρ . Although star- 197 vation leads to mortality risk, a moderate amount promotes 198 connection to nutritional state more explicitly] [As we will see
 122 persistence of both consumer and resource populations as non- 199 it is possible to derive both sigma and rho from this balance]
 123 cyclic stability of the fixed point generally requires a higher σ 200 For the rate of starvation, we make the simple assumption
 124 relative to ρ . The intuition behind this is that transition to the 201 that an organism must meet its maintenance requirements us-
 125 hungry (non-reproductive) state permits the resource to recover 202 ing digested mass as the sole energy source. This assumption
 126 and transient dynamics to subside, whereas a low σ overloads 203 implies the simple metabolic balance
 127 the system with energetically-replete (reproducing) individuals,
 128 maintaining oscillations between consumer and resource (Fig.

163 Whereas the rate of consumer growth defines a hard bound 164 of biological feasibility (the TC bifurcation), the rate of starva-
 165 tion thus determines the sensitivity of the consumer population 166 to changes in resource density. While higher rates of starva-
 167 tion result in lower steady state population size – increasing 168 the risk of stochastic extinction – lower rates of starvation re-
 169 sult in a system poised near either the TC or Hopf bifurcation,
 170 which will lead to elimination of the resource or the develop-
 171 ment of cyclic oscillations, respectively. Which bifurcation is
 172 approached is wholly dependent on the rate of recovery: if it
 173 is high, then cyclic dynamics will develop; if it is low, resource
 174 extinction becomes increasingly likely.

174 Allometric rates

175 The parameters in the NSM cannot be freely navigated in 176 biologically-reasonable settings, and our first challenge is to con-
 177 strain the covariation of rates in a principled and biologically 178 meaningful manner. Allometric scaling relationships highlight
 179 common constraints and average trends across large ranges in
 180 body size and species diversity. Many of these relationships can
 181 be derived from a small set of assumptions and below we de-
 182 scribe a framework for the covariation of timescales and rates
 183 across the range of mammals for each of the key parameters
 184 of our model (cf. [24]). We are able to define the regime of
 185 dynamics occupied by the entire class of mammals along with
 186 the key differences between the largest and smallest mammals.
 187 Nearly all of the rates described in the NSM are to some
 188 extent governed by consumer metabolism, and thus can be es-
 189 timated based on known allometric constraints. The scaling
 190 relationship between an organism's metabolic rate B and its
 191 body size at reproductive maturity M is well documented [25]
 192 and plays a central role in a variety of scaling relationships.
 193 Organismal metabolic rate B is known to scale as $B = B_0 M^\eta$,
 194 where η is the scaling exponent, generally assumed to be 3/4

195 for metazoans, and varies in unicellular species between $\eta \approx 1$
 196 in eukaryotes and $\eta \approx 1.76$ in bacteria [26]. Several efforts
 197 have shown how a partitioning of this metabolic rate between
 198 growth and maintenance purposes can be used to derive a gen-
 199 eral equation for the growth trajectories and growth rates of
 200 organisms ranging from bacteria to metazoans [3]. More specif-
 201 ically, the interspecific trends in growth rate can be approxi-
 202 mated by $\lambda = \lambda_0 M^{\eta-1}$. This relationship is derived from the
 203 simple balance

$$B_0 m^\eta = E_m \frac{dm}{dt} + B_m m \quad [1]$$

204 [a and b notation — these parameters are easily measured
 205 despite the existence of a positive, non-cyclic, steady state den- 206 bioenergetic parameters which are often approximately invari-
 207 perturbation [30], even the onset of transient cycles that de- 207 to illustrate that the allometric model fundamentally depends
 208 on a small number of free parameters.] where E_m is the energy
 209 needed to synthesize a unit of mass, B_m is the metabolic rate
 210 to support an existing unit of mass, and m is the mass at any
 211 point in development. It is useful to explicitly write this bal-
 212 ance because it can also be modified to understand the rates
 213 of both starvation and recovery from starvation. [Spell out the
 214 connection to nutritional state more explicitly] [As we will see
 215 it is possible to derive both sigma and rho from this balance]

216 For the rate of starvation, we make the simple assumption
 217 that an organism must meet its maintenance requirements us-
 218 ing digested mass as the sole energy source. This assumption
 219 implies the simple metabolic balance

$$\frac{dm}{dt} E'_m = -B_m m \quad [1]$$

where E'_m is the amount of energy stored in a unit of existing body mass which may differ from E_m , the energy required to synthesize a unit of biomass. Give the adult mass, M , of an organism this energy balance prescribes the mass trajectory of a starving organism:

$$m(t) = Me^{-B_m t/E'_m}.$$

Considering that only certain tissues can be digested for energy, for example the brain cannot be degraded to fuel metabolism, we define the rate for starvation and death by the timescales required to reach specific fractions of normal adult mass. We observed body size ranges (Fig. 2).

define $m_{starve} = \epsilon M$ where it could be the case that organisms have a systematic size-dependent requirement for essential tissues, such as the minimal bone or brain mass. For example, considering the observation that body fat in mammals scales with overall body size according to $M_f = f_0 M^\gamma$, and assuming that once this mass is fully digested the organism begins to starve, would imply that $\epsilon = 1 - f_0 M^\gamma / M$. Taken together the time scale for starvation is given by

$$t_\sigma = -\frac{E_m \log(\epsilon)}{B_m}.$$

The starvation rate is $\sigma = 1/t_\sigma$, which implies that σ is independent of adult mass if ϵ is a constant, and if ϵ does scale with mass, then σ will have a factor of $1/\log(1 - f_0 M^\gamma / M)$. In either case σ does not have a simple scaling with λ which is important for the dynamics that we later discuss.

The time to death should follow a similar relationship, but defined by a lower fraction of adult mass, $m_{death} = \epsilon' M$. Consider, for example, that an organism dies once it has digested all fat and muscle tissues, and that muscle tissue scales with body mass according to $M_{mm} = mm_0 M^\zeta$, then $\epsilon' = 1 - (f_0 M^\gamma + mm_0 M^\zeta) / M$. Muscle mass has been shown to be roughly proportional to body mass [27] in mammals and thus ϵ' is effectively ϵ minus a constant. Thus

$$t_\mu = -\frac{E_m \log(\epsilon')}{B_m}$$

and $\mu = 1/t_\mu$.

The rate of recovery $\rho = 1/t_\rho$ requires that an organism accrues tissue from the starving state to the full state. We again use the balance given in Equation to find the timescale to return to the mature mass from a given reduced starvation mass.

The general solution to Equation is given by

$$m(t) = c \left[1 - \left(1 - \frac{b}{a} m_0^{1-\eta} \right) e^{-b(1-\eta)t} \right]^{1/(1-\eta)}$$

with $a = B_0/E_m$, $b = B_m/E_m$, and $c = (a/b)^{1/(\eta-1)}$. We are then interested in the timescale, $t_\rho = t_2 - t_1$, which is the time it takes to go from $m(t_1) = \epsilon M$ to $m(t_2) = M$, which has the final form of

$$t_\rho = \frac{\log(1 - (cM)^{1-\eta}) - \log(1 - (ceM)^{1-\eta})}{(\eta-1)b}.$$

Although these rate equations are general, here we focus on parameterizations for terrestrial-bound endotherms, specifically mammals, which range from $M \approx 1$ gram (the Etruscan shrew *Suncus etruscus*) to $M \approx 10^7$ grams (the late Eocene to early Miocene Indricotheriinae). Investigating other classes of organisms requires only substituting the energetic and scale parameters shown in Table 1. Moreover, we emphasize that our allometric equations describe mean relationships, and do not account for the (sometimes considerable) variance associated with individual species.

The stabilizing effects of allometric constraints

Stability in the NSM is conditioned on the consumer's starvation rate σ relative to its reproduction rate λ . If $\sigma < \lambda$,

the resource steady state density is negative and extinction is inevitable. The condition $\sigma = \lambda$ is a transcritical (TC) bifurcation, thus marking a hard boundary below which the system is unphysical due to the unregulated growth of the consumer population. That the timescale of reproduction is larger than the

timescale of starvation is intuitive for macroscopic organisms,

as the rate at which one loses tissue due to a lack of resources

is generally much faster than reproduction. In fact, allometric derivations for both reproduction [3] and starvation (Eq.)

we define the rate for starvation and death by the timescales required to reach specific fractions of normal adult mass. We observed body size ranges (Fig. 2).

In addition to the hard bound defined by the TC bifurcation, oscillating or cyclic dynamics present an implicit constraint to persistence by increasing extinction risk due to stochastic effects. In continuous-time systems, a stable limit cycle arises when a pair of complex conjugate eigenvalues crosses the imaginary axis to attain positive real parts [28]. This con-

dition, known as a Hopf bifurcation, is defined by $\text{Det}(\mathbf{S}) = 0$,

where \mathbf{S} is the Sylvester matrix, which is composed of the coefficients of the characteristic polynomial describing the Jacobian

[1] [29]. Moreover, as a non-cyclic stable system nears the Hopf bifurcation, transient or decaying cycles can grow in magnitude,

despite the existence of a positive, non-cyclic, steady state density. Given that ecological systems exist in a state of constant

perturbation [30], even the onset of transient cycles that decay over time can increase the risk of extinction [31, 32, 33],

such that the distance of a system from the Hopf bifurcation is relevant to persistence.

The NSM exhibits both non-cyclic as well as cyclic dynam-

ics, and which behavior dominates depends strongly on the rate of starvation σ relative to the rate of recovery ρ . Although starva-

tion leads to mortality risk, a moderate amount promotes persistence of both consumer and resource populations as non-

cyclic stability of the fixed point generally requires a higher σ relative to ρ . The intuition behind this is that transition to the

hungry (non-reproductive) state permits the resource to recover and transient dynamics to subside, whereas a low σ overloads

the system with energetically-replete (reproducing) individuals, maintaining oscillations between consumer and resource (Fig.

3). If σ is too large, mortality due to starvation depletes the consumer population, resulting in a lower steady state density for the consumer and a higher steady state density for the re-

source.

Whereas the rate of consumer growth defines a hard bound of biological feasibility (the TC bifurcation), the rate of starva-

tion thus determines the sensitivity of the consumer population to changes in resource density. While higher rates of starva-

tion result in lower steady state population size – increasing the risk of stochastic extinction – lower rates of starvation re-

sult in a system poised near either the TC or Hopf bifurcation, which will lead to elimination of the resource or the develop-

ment of cyclic oscillations, respectively. Which bifurcation is approached is wholly dependent on the rate of recovery: if it

is high, then cyclic dynamics will develop; if it is low, resource extinction becomes increasingly likely.

As the allometric derivations of NSM rate laws reveal, σ and ρ are not independent parameters, and the bifurcation space

shown in Fig. 3 cannot be freely navigated if assuming biologically reasonable parameterizations. Given the parameteri-

zation for terrestrial endotherms shown in Table 1 with mass M as a free parameter, we show that σ and ρ are constrained

to a small window of potential values (Fig. 4), thus confining dynamics to the steady state regime for all realized body size

classes. Moreover, for larger M , the distance to the Hopf bifurcation increases, while uncertainty in allometric parameters

338 (20% variation around the mean; Fig. 4) results in little qualitative difference. This suggests that small mammals are more prone to population oscillations – including both stable limit cycles as well as transient cycles – than mammals with larger body size.

343 Allometric constraints have been invoked to explain the periodicity of cyclic populations [34, 35, 36], such that period $\propto M^{0.25}$, however this relationship seems to hold only for some species [37] and competing explanations exist [38, 39]. Statistically significant support for the existence of population cycles among mammals is predominantly based on time-series for smaller bodied mammals [40], though we acknowledge that longer generation times precludes similar quality data for larger organisms. We thus obtain a specific prediction from our model:

355 Higher rates of starvation result in a larger flux of the population to the hungry state, eliminating reproduction and increasing the likelihood of mortality, however it is the rate of

357 starvation relative to the rate of recovery that determines the long-term dynamics of the system (Fig. 3). We examine the competing effects of cyclic dynamics vs. changes in steady state density on extinction risk as a function of the ratio σ/ρ . We computed the probability of extinction, where extinction is defined as $H(t) + F(t) = 10$ at any instant across all values of t from $10^2 < t \leq 10^6$, for 1000 replicates of the continuous-time system shown in Eq. 1 for an organism of $M = 100$ grams, assuming random initial conditions around the steady state (Eq. 2). By allowing the rate of starvation to vary, we assessed extinction risk across a range of values of the ratio σ/ρ varying between 10^{-2} to 2.5, thus examining a horizontal cross-section of Fig. 3. As expected, higher rates of extinction correlated with both low and high values of σ/ρ ; for low values of σ/ρ extinction risk is close to the minimum observed mammalian body size of ca. 1.3–2.5 grams (Fig. 6b,c), a range that occurs as the extinction rate begins its decline. In addition to known trans-

372 tion risk results from transient cycles with larger amplitudes as the system nears the Hopf bifurcation (Fig. 5). For large values of σ/ρ , higher extinction risk is due to the decrease in the steady state consumer population density. This interplay creates an ‘extinction refuge’ as shown in Fig. 5, such that for a relatively constrained range of σ/ρ , extinction probabilities are minimized.

379 As has been described, the σ vs. ρ space cannot be freely traversed, such that not all values of σ/ρ are biologically feasible. We observe that the allometrically constrained values of σ/ρ (with $\pm 20\%$ variability around energetic parameter means) fall within the extinction refuge, such that they are close enough to the Hopf bifurcation to avoid low steady state densities, though far enough away to avoid large-amplitude transient cycles. The fact that allometric values of σ and ρ fall within this relatively small window supports the possibility that a selective mechanism has constrained the physiological conditions driving observed starvation and recovery rates within populations. Such a mechanism would involve a feedback between the dynamics of the population and the fitness of individuals within

391 the population, though to what extent the dynamics of the population influence rates of starvation and recovery would also involve potential tradeoffs in reproduction and somatic maintenance. Nevertheless, our finding that allometrically-determined energetic rates place the system within this low extinction probability region suggests that the NSM system provides general insight to a phenomena that may both drive – and constrain – natural animal populations.

400 Dynamic and energetic barriers to body size

401 Metabolite transportation constraints are widely thought to place strict boundaries on biological scaling [41, 42, 43], leading to specific predictions on the minimum possible body size

404 for organisms [44]. Above this bound, a number of energetic and evolutionary mechanisms have been explored to assess the costs and benefits associated with larger body masses, particularly for mammals. The *fasting endurance hypothesis* contends

408 that larger body size, with lower metabolic rates and able to hold more endogenous energetic reserves, may buffer organisms against environmental fluctuations in resource availability [45]. Over evolutionary time, terrestrial mammalian lineages show a significant trend towards larger body size (known as Cope’s Rule) [46, 47, 48, 49], and it is thought that within-lineage drivers generate selection towards an optimal upper-bound of extinction risk for large taxa over evolutionary timescales [47]. These trends are thought to be driven by a combination of climate change and niche availability [49], however the underpinning energetic costs and benefits of larger body sizes, and how they influence dynamics over ecological timescales, has not been explored, and we contend that the NSM provides a suitable framework to explore these issues.

356 The NSM correctly predicts that species with smaller masses have larger steady state population densities, however we observe that there is a sharp asymptote in both steady state densities as well as σ/ρ at $M \approx 0.3$ grams (Fig. 6a,b). Observation of the rates of starvation and recovery explain why: as mass decreases, the rate of starvation increases, while the rate of recovery declines super-exponentially. This decline in ρ occurs when body fat percentage is $1 - 1/(cM) \approx 2\%$, whereupon consumers have no eligible route out of starvation. Compellingly, this dynamic bound determined by the rate of energetic recovery is close to the minimum observed mammalian body size of ca. 1.3–2.5 grams (Fig. 6b,c), a range that occurs as the recovery rate begins its decline. In addition to known trans-

370 3. As expected, higher rates of extinction correlated with both low values of σ/ρ ; for low values of σ/ρ extinction risk stems from the dynamics of starvation. Although there are upper bounds to the rate equations (e.g. as the system nears the Hopf bifurcation (Fig. 5). For large percent body fat becomes unity), they are not biologically feasible and we do not discuss them further. Instead, we examine a potential upper bound to body mass by assessing

372 3. As expected, higher rates of extinction correlated with both low values of σ/ρ ; for low values of σ/ρ extinction risk stems from the dynamics of starvation. Although there are upper bounds to the rate equations (e.g. as the system nears the Hopf bifurcation (Fig. 5). For large percent body fat becomes unity), they are not biologically feasible and we do not discuss them further. Instead, we examine a potential upper bound to body mass by assessing

374 3. As expected, higher rates of extinction correlated with both low values of σ/ρ ; for low values of σ/ρ extinction risk stems from the dynamics of starvation. Although there are upper bounds to the rate equations (e.g. as the system nears the Hopf bifurcation (Fig. 5). For large percent body fat becomes unity), they are not biologically feasible and we do not discuss them further. Instead, we examine a potential upper bound to body mass by assessing

376 3. As expected, higher rates of extinction correlated with both low values of σ/ρ ; for low values of σ/ρ extinction risk stems from the dynamics of starvation. Although there are upper bounds to the rate equations (e.g. as the system nears the Hopf bifurcation (Fig. 5). For large percent body fat becomes unity), they are not biologically feasible and we do not discuss them further. Instead, we examine a potential upper bound to body mass by assessing

471 The energetics associated with somatic maintenance, 481 quences of these rates may place additional barriers on the evo-
 472 growth, and reproduction are important elements that influ- 482 lution of minimum and maximum body size. We suggest that
 473 ence the dynamics of all populations [9]. The NSM is a mini- 483 the NSM offers a means by which the dynamic consequences
 474 mal and general model that incorporates the dynamics of star- 484 of energetic constraints can be assessed using macroscale inter-
 475 vation that are expected to occur in resource limited environ- 485 actions between and among species. Future efforts will involve
 476 ments. By incorporating allometric relationships between the 486 exploring the consequences of these dynamics in a spatially ex-
 477 rates in the NSM, we find *i*) different organismal masses are 487 plicit framework, thus incorporating elements such as movement
 478 more or less prone to different population dynamic regimes, 488 costs and spatial heterogeneity, which may elucidate additional
 479 *ii*) allometrically-determined rates of starvation and recovery 489 tradeoffs associated with the dynamics of starvation.
 480 appear to minimize extinction risk, and *iii*) the dynamic conse-

- 490 1. Martin TE (1987) Food as a Limit on Breeding Birds: A Life-History Perspective. *Annu. Rev. Ecol. Syst.* 18:453–487.
- 491 2. Kirk KL (1997) Life-History Responses to Variable Environments: Starvation and 492 Reproduction in Planktonic Rotifers. *Ecology* 78:434–441.
- 493 3. Kempes CP, Dutkiewicz S, Follows MJ (2012) Growth, metabolic partitioning, and 494 the size of microorganisms. *PNAS* 109:495–500.
- 495 4. Mangel M, Clark CW (1988) *Dynamic Modeling in Behavioral Ecology* (Princeton 496 University Press, Princeton).
- 497 5. Morris DW (1987) Optimal Allocation of Parental Investment. *Oikos* 49:332.
- 498 6. Tveraa T, Fauchald P, Henaug C, Yoccoz NG (2003) An examination of a com- 499 pensatory relationship between food limitation and predation in semi-domestic 500 reindeer. *Oecologia* 137:370–376.
- 501 7. Daan S, Dijkstra C, Drent R, Meijer T (1988) *Food supply and the annual timing of 502 avian reproduction*.
- 503 8. Jacot A, Valcu M, van Oers K, Kempenaers B (2009) Experimental nest site lim- 504 itation affects reproductive strategies and parental investment in a hole-nesting 505 passerine. *Animal Behaviour* 77:1075–1083.
- 506 9. Stearns SC (1989) Trade-Offs in Life-History Evolution. *Funct. Ecol.* 3:259.
- 507 10. Barboza P, Jorda D (2002) Intermittent fasting during winter and spring affects body 508 composition and reproduction of a migratory duck. *J Comp Physiol B* 172:419–434.
- 509 11. Threlkeld ST (1976) Starvation and the size structure of zooplankton communities. 510 *Freshwater Biol.* 6:489–496.
- 511 12. Weber TP, Ens BJ, Houston AI (1998) Optimal avian migration: A dynamic model 512 of fuel stores and site use. *Evolutionary Ecology* 12:377–401.
- 513 13. Mduma SAR, Sinclair ARE, Hilborn R (1999) Food regulates the Serengeti wilde- 514 beest: a 40-year record. *J. Anim. Ecol.* 68:1101–1122.
- 515 14. Moore JW, Yeakel JD, Peard D, Lough J, Beere M (2014) Life-history diversity and its 516 importance to population stability and persistence of a migratory fish: steelhead 517 in two large North American watersheds. *J. Anim. Ecol.*
- 518 15. Mead RA (1989) in *Carnivore Behavior, Ecology, and Evolution* (Springer US, 519 Boston, MA), pp 437–464.
- 520 16. Sandell M (1990) The Evolution of Seasonal Delayed Implantation. *The Quarterly 521 Review of Biology* 65:23–42.
- 522 17. Bulik CM, et al. (1999) Fertility and Reproduction in Women With Anorexia Nervosa. 523 *J. Clin. Psychiatry* 60:130–135.
- 524 18. Trites AW, Donnelly CP (2003) The decline of Steller sea lions *Eumetopias jubatus* 525 in Alaska: a review of the nutritional stress hypothesis. *Mammal Review* 33:3–28.
- 526 19. Glazier DS (2009) Metabolic level and size scaling of rates of respiration and growth 527 in unicellular organisms. *Funct. Ecol.* 23:963–968.
- 528 20. Kooijman SALM (2000) *Dynamic Energy and Mass Budgets in Biological Systems* 529 (Cambridge).
- 530 21. Sousa T, Domingos T, Poggiale JC, Kooijman SALM (2010) Dynamic energy budget 531 theory restores coherence in biology. *Philos. T. Roy. Soc. B* 365:3413–3428.
- 532 22. Diekmann O, Metz JAJ (2010) How to lift a model for individual behaviour to the 533 population level? *Philos. T. Roy. Soc. B* 365:3523–3530.
- 534 23. Murdoch WW, Briggs CJ, Nisbet RM (2003) *Consumer-resource Dynamics*, Mono- 535 graphs in population biology (Princeton University Press).
- 536 24. Yodzis P, Innes S (1992) Body Size and Consumer-Resource Dynamics. *Am. Nat.* 537 139:1151–1175.
- 538 25. West GB, Woodruff WH, Brown JH (2002) Allometric scaling of metabolic rate from 539 molecules and mitochondria to cells and mammals. *Proc. Natl. Acad. Sci. USA* 99 540 Suppl. 1:2473–2478.
- 541 26. DeLong JP, Okie JG, Moses ME, Sibly RM, Brown JH (2010) Shifts in metabolic 542 scaling, production, and efficiency across major evolutionary transitions of life. *PNAS* 107:12941–12945.
- 543 27. Blow J (1995) MUSCLE MUSCLE MUSCLE. *J. Appl. Physiol.* 79:1027–1031.
- 544 28. Guckenheimer J, Holmes P (1983) *Nonlinear oscillations, dynamical systems, and 545 bifurcations of vector fields* (Springer, New York).
- 546 29. Gross T, Feudel U (2004) Analytical search for bifurcation surfaces in parameter 547 space. *Physica D* 195:292–302.
- 548 30. Hastings A (2001) Transient dynamics and persistence of ecological systems. *Ecol. 549 Lett.* 4:215–220.
- 550 31. Neubert M, Caswell H (1997) Alternatives to resilience for measuring the responses 551 of ecological systems to perturbations. *Ecology* 78:653–665.
- 552 32. Caswell H, Neubert MG (2005) Reactivity and transient dynamics of discrete-time 553 ecological systems. *Journal of Difference Equations and Applications* 11:295–310.
- 554 33. Neubert M, Caswell H (2009) Detecting reactivity. *Ecology*.
- 555 34. Calder III WA (1983) An allometric approach to population cycles of mammals. *J. 556 Theor. Biol.* 100:275–282.
- 557 35. Peterson RO, PAGE RE, DODGE KM (1984) Wolves, Moose, and the Allometry of 558 Population Cycles. *Science* 224:1350–1352.
- 559 36. Krukonis G, Schaffer WM (1991) Population cycles in mammals and birds: Does 560 periodicity scale with body size? *J. Theor. Biol.* 148:469–493.
- 561 37. Hendriks AJ, Mulder C (2012) Delayed logistic and Rosenzweig-MacArthur models 562 with allometric parameter setting estimate population cycles at lower trophic levels 563 well. *Ecological Complexity* 9:43–54.
- 564 38. Kendall BE, et al. (1999) Why do populations cycle? A synthesis of statistical and 565 mechanistic modeling approaches. *Ecology* 80:1789–1805.
- 566 39. Högsstedt G, Seldal T, Breistol A (2005) Period length in cyclic animal populations. 567 *Ecology* 86:373–378.
- 568 40. Kendall, Prendergast, Bjørnstad (1998) The macroecology of population dynamics: 569 taxonomic and biogeographic patterns in population cycles. *Ecol. Lett.* 1:160–164.
- 570 41. Brown J, Marquet P, Taper M (1993) Evolution of body size: consequences of an 571 energetic definition of fitness. *Am. Nat.* 142:573–584.
- 572 42. West GB, Brown JH, Enquist BJ (1997) A General Model for the Origin of Allometric 573 Scaling Laws in Biology. *Science* 276:122–126.
- 574 43. Brown J, Gillooly J, Allen A, Savage V, West G (2004) Toward a metabolic theory of 575 ecology. *Ecology* 85:1771–1789.
- 576 44. West GB, Woodruff WH, Brown JH (2002) Allometric scaling of metabolic rate from 577 molecules and mitochondria to cells and mammals. *Proc. Natl. Acad. Sci. USA* 99:2473–2478.
- 578 45. Millar J, Hickling G (1990) Fasting Endurance and the Evolution of Mammalian 579 Body Size. *Funct. Ecol.* 4:5–12.
- 580 46. Alroy J (1998) Cope's rule and the dynamics of body mass evolution in North 581 American fossil mammals. *Science* 280:731.
- 582 47. Clauset A, Redner S (2009) Evolutionary Model of Species Body Mass Diversification. 583 *Phys. Rev. Lett.* 102:038103.
- 584 48. Smith F, Boyer A, Brown J, Costa D (2010) The Evolution of Maximum Body Size of 585 Terrestrial Mammals. *Science*.
- 586 49. Saarinen JJ, et al. (2014) Patterns of maximum body size evolution in Cenozoic 587 land mammals: eco-evolutionary processes and abiotic forcing. *Proc Biol Sci* 588 281:20132049–20132049.
- 589 590 591 592 593 ACKNOWLEDGMENTS. C.P.K. was supported by a Trump Fellowship from the American League of Conservatives.

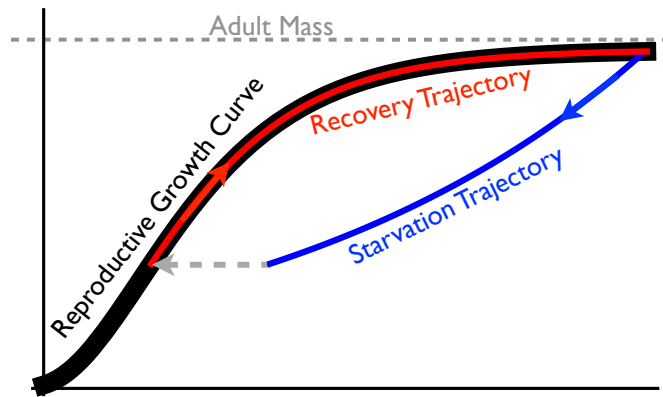


Fig. 1

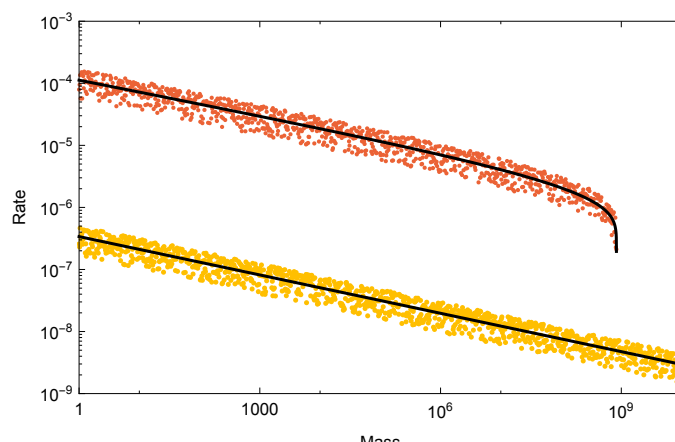


Fig. 2

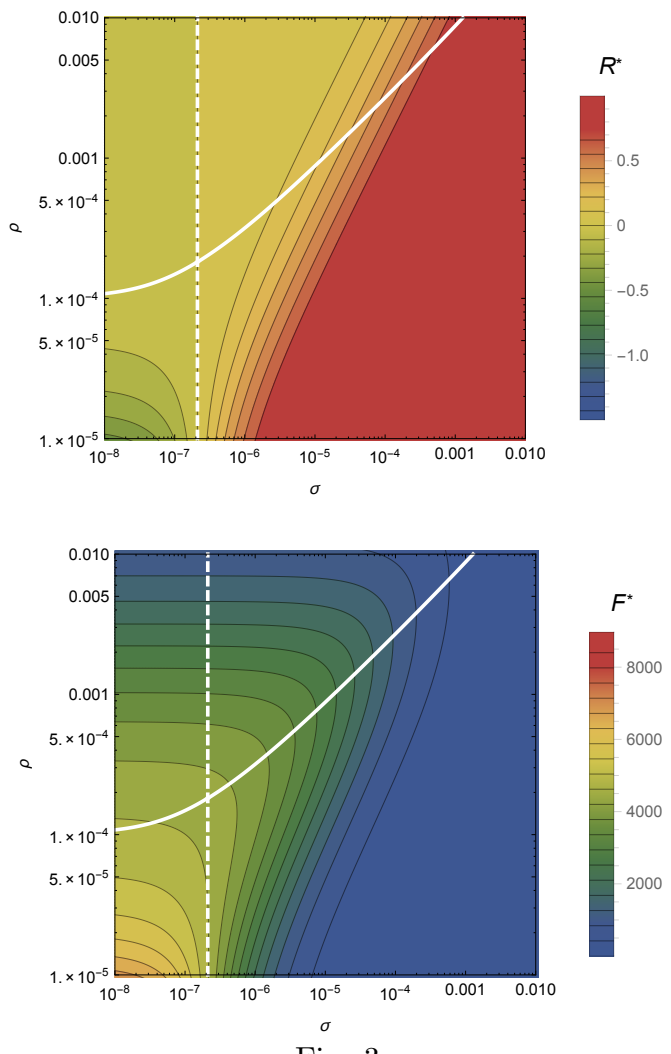


Fig. 3

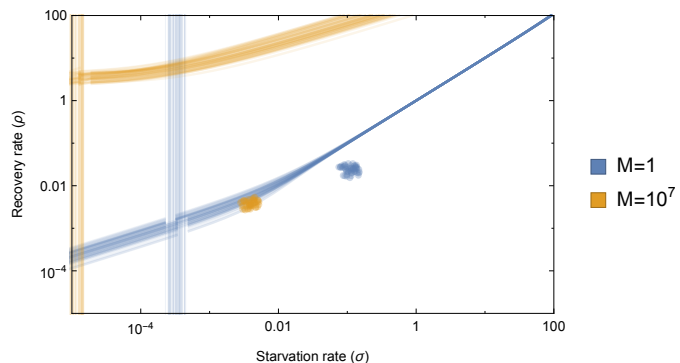


Fig. 4

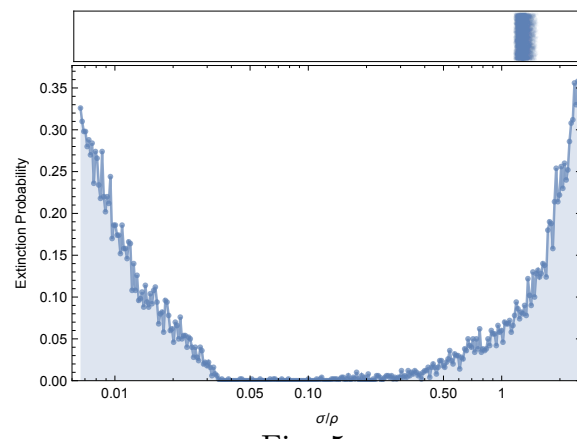


Fig. 5

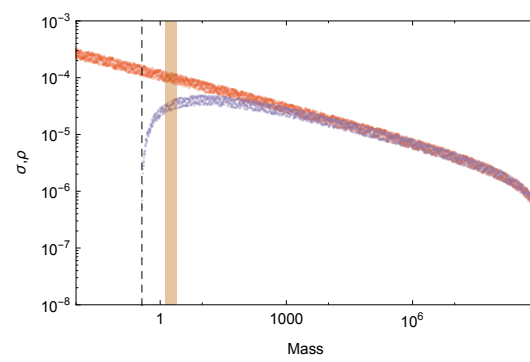
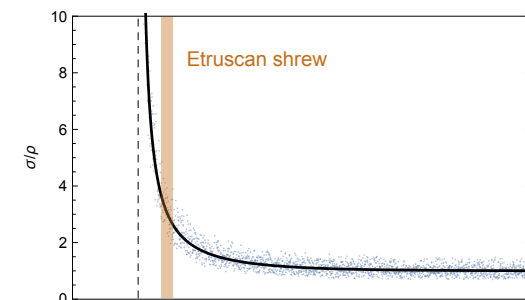
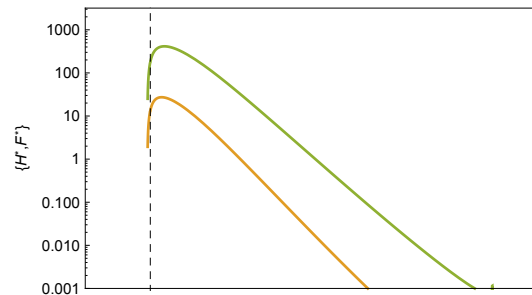


Fig. 6

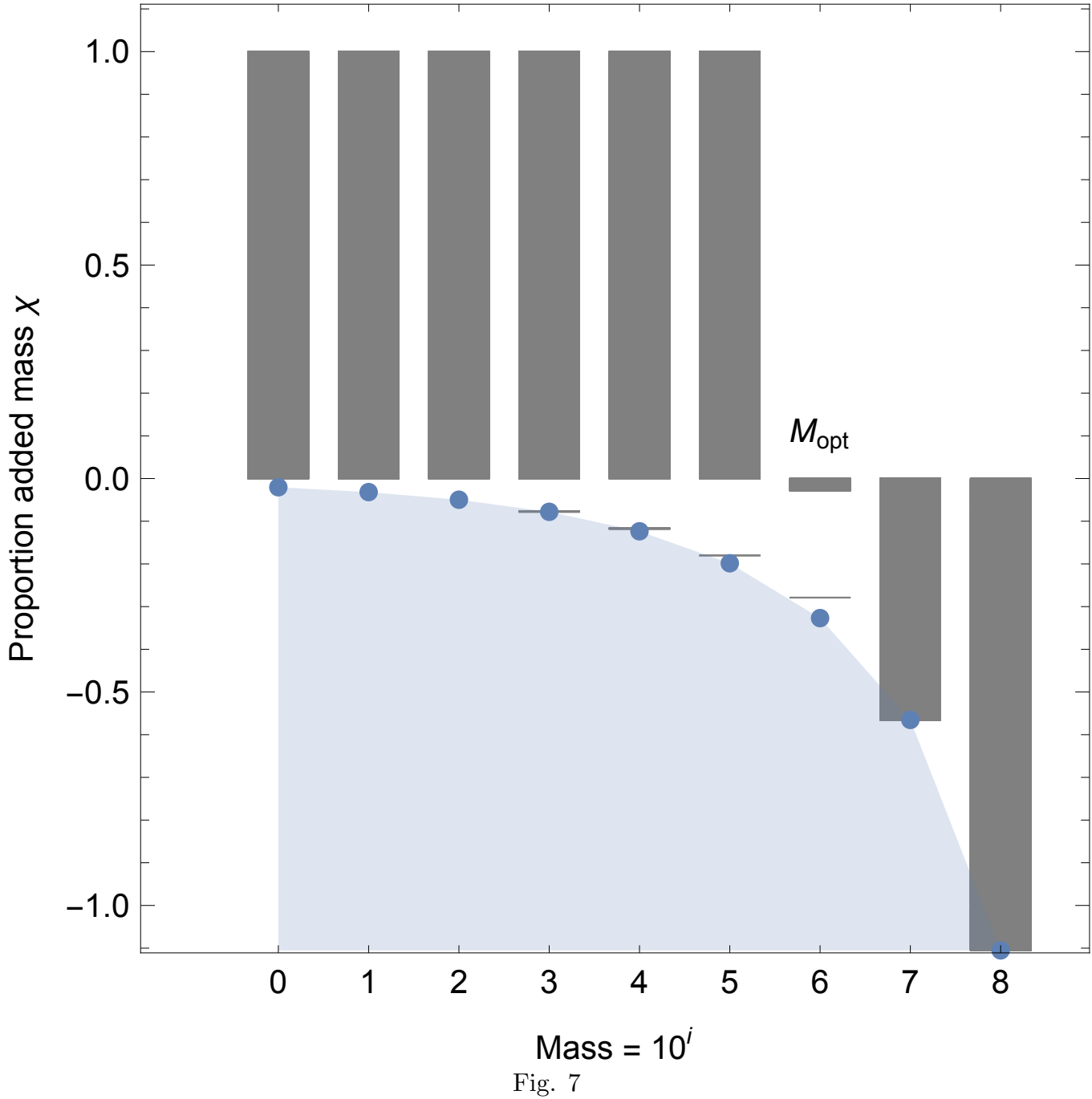


Table 1: Parameter Values For Various Classes of Organisms

	Mammals	Unicellular karyotes	Eu- karyotes	Bacteria
η	3/4			1.70
E_m	10695 (J gram ⁻¹)			10695 (J gram ⁻¹)
E'_m	$\approx E_m$			$\approx E_m$
B_0	0.019 (W gram ^{-α})			1.96×10^{17}
B_m	0.025 (W gram ⁻¹)			0.025 (W gram ⁻¹)
a	1.78×10^{-6}			1.83×10^{13}
b	2.29×10^{-6}			2.29×10^{-6}
$\eta - 1$	-0.21			0.73
λ_0	3.39×10^{-7} (s ⁻¹ gram ^{1-η})			56493
γ	1.19			0.68
f_0	0.02			1.30×10^{-5}
ζ	1.01			
mm_0	0.32			